ORGANOMETALLICS

Communication

pubs.acs.org/Organometallics

Formation of η^2-Coordinated Dihydropyridine–Ruthenium(II) Complexes by Hydride Transfer from Ruthenium(II) to Pyridinium Cations

Yasuo Matsubara,[†,‡] Tatsumi Kosaka,[§] Kichitaro Koga,[∥] Akira Nagasawa,[§] Atsuo Kobayashi,[§] Hideo Konno,[§,⊥] Carol Creutz,[†] Kazuhiko Sakamoto,[§] and Osamu Ishitani*[,∥]

[†]Chemistry Department, Brookhaven National Laboratory, Upton, New York 11973-5000, United States

[‡]PRESTO, Japan Science and Technology Agency (JST), Chiyoda-ku, Tokyo 102-0076, Japan

[§]Graduate School of Science and Engineering, Saitama University, 255 Shimo-Okubo, Saitama 338-8570, Japan

[∥]Department of Chemistry, Graduate School of Science and Engineering, Tokyo Institute of Technology, O-okayama 2-12-1-NE-1, Meguro-ku, Tokyo 152-8550, Japan

Supporting Information

ABSTRACT: Reactions between various pyridinium cations with and without a $-CF_3$ substituent at the 3-position and $[Ru(tpy)(bpy)H]^+$ (tpy = 2,2′:6′,2″-terpyridine and bpy = 2,2′-bipyridine) were investigated in detail. The corresponding 1,4-dihydropyridines coordinating to a Ru(II) complex in η^2 mode through a C═C bond were quantitatively formed at the initial stage. The only exception observed was in the case of the 1-benzylpyridinium cation, where a mixture of two adducts with 1,4-dihydropyridine and 1,2-dihydropyridine was formed in the ratio 96:4. Cleavage of the Ru–(C═C) bond proceeded at a slower rate in all reactions, giving the corresponding dihydropyridine and $[Ru(tpy)(bpy)(NCCH_3)]^{2+}$ when acetonitrile was used as a solvent. Kinetic activation parameters for the adduct formation indicated that the 1,4-regioselectivities were induced by formation of sterically constrained structures.

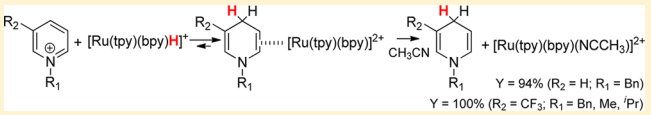

Hydride reduction of pyridinium cation to dihydropyridine is an important elemental step in biological redox systems, i.e., conversion of coenzyme $NAD(P)^+$ to NAD(P)H,[1] and in the preparation of various synthons used in heterocyclic synthesis.[2] Factors that control the positions of the ring at which a hydride attacks have attracted particular interest.[3] Transition-metal hydride and formyl complexes of Ru(II),[4] Re(I),[4c,5] Rh(III),[6] and Ir(III)[7] have been established as hydride donors for the reduction of pyridinium-type cations. In some cases, a carbamoyl group, which is a substituent at the 3-position of the ring in the $NAD(P)^+$ models, has been thought to play an important role as a directing group to induce 1,4-regioselectivity.[4a,c,6b] For instance, we found that a Ru complex coordinated by the carbamoyl group of 1-benzyl-1,4-dihydronicotinamide (BNAH), i.e., $[Ru(tpy)(bpy)(BNAH)]^{2+}$ (**RuBNAH**$^{2+}$; tpy = 2,2′:6′,2″-terpyridine and bpy = 2,2′-bipyridine) was produced as an important intermediate of 1,4-regioselective hydride reduction of 1-benzyl-3-carbamoylpyridinium cation (BNA^+) by $[Ru(tpy)(bpy)H]^+$ (**RuH**$^+$).[4c] This strongly suggests that the interaction between the carbamoyl group of BNA^+ and the central metal of the Ru complex is an important factor in the 1,4-regioselectivity. Fish et al. also have suggested the importance of a similar interaction in the hydride reduction of $NAD(P)^+$ models with $[Cp^*Rh(bpy)H]^+$ (**RhH**$^+$; Cp^* = pentamethylcyclopentadienyl).[6b,c] Reduction of 1-benzyl-3-acetylpyridinium cation ($BAcPy^+$), bearing an acetyl group instead of the carbamoyl group of BNA^+, by **RuH**$^+$[4c] or **RhH**$^+$[6b,c] selectively gave the corresponding 1,4-dihydro form (1,4-BAcPyH) and 1:1 adduct $[Ru(tpy)(bpy)(1,4\text{-BAcPyH})]^{2+}$, which was identified when **RuH**$^+$ was used. Therefore, the carbonyl group should be able to interact with the metal center of the hydride complexes in the transition state(s). Moreover, Fish et al. reported that pyridinium cation with a noncoordinating group such as methyl at the 3-position could not be reduced by **RhH**$^+$.

Herein, we report reactions of **RuH**$^+$ with pyridinium cations without a substituent or with a noncoordinating group ($-CF_3$) at the 3-position of the pyridinium ring (Scheme 1). These cations could react with **RuH**$^+$ to give the corresponding dihydro form(s), and we found that new types of Ru(II)-bound η^2-1,4-dihydropyridine adducts are formed during these reactions (Scheme 1).

Scheme 1. Formation of the Reaction Intermediates in the Reactions of Pyridinium Cations with RuH$^+$

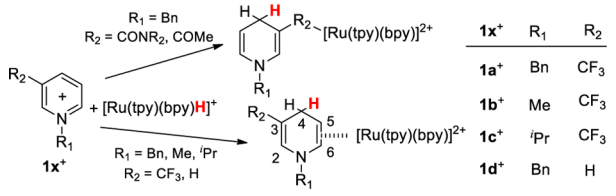

1x$^+$	R_1	R_2
1a$^+$	Bn	CF_3
1b$^+$	Me	CF_3
1c$^+$	^{i}Pr	CF_3
1d$^+$	Bn	H

Received: August 30, 2013
Published: October 29, 2013

dx.doi.org/10.1021/om400862n | *Organometallics* 2013, 32, 6162–6165

In a typical run, PF_6^- salts of 1-benzyl-3-trifluoromethylpyridinium cation ($\mathbf{1a}^+$; 15 μmol) and $\mathbf{RuH}^+$ (15 μmol) were dissolved in 0.7 mL of acetonitrile-d_3 at room temperature. Quantitative formation of the corresponding 1,4-dihydro form of $\mathbf{1a}^+$ ($\mathbf{1aH(1,4)}$) and a solvento complex, $[Ru(tpy)(bpy)(NCCH_3)]^{2+}$ ($\mathbf{RuAN}^{2+}$), was observed within 5 min (eq 1).

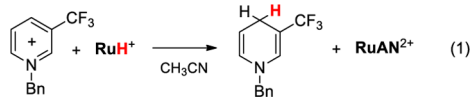

The formation of positional isomers, i.e., 1,2- and 1,6-dihydro isomers, and one-electron-reduced dimers ($\mathbf{1a}_2$) was not observed in the ^{1}H NMR spectrum of the sample prepared at room temperature (Figure 1b). We could detect the

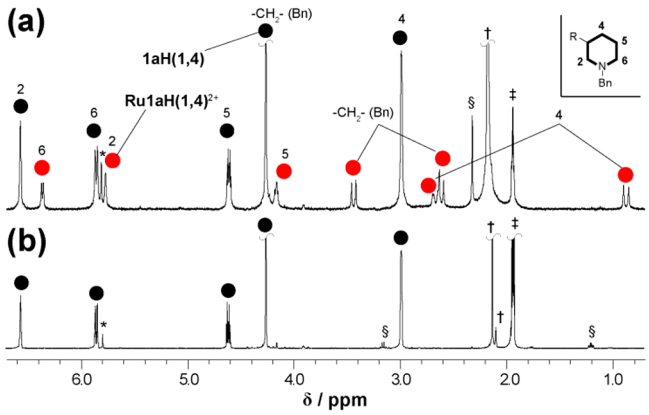

Figure 1. ^{1}H NMR spectra measured (a) at low temperature (red ●, $\mathbf{Ru1aH(1,4)}^{2+}$; black ●, $\mathbf{1aH(1,4)}$) and (b) at room temperature after mixing $\mathbf{RuH}^+$ (15 μmol) and $\mathbf{1a}^+$ (15 μmol) in acetonitrile-d_3 (0.7 mL). The peaks marked with *, †, ‡, and § are attributed to excess $\mathbf{1a}^+$, water, residual solvent protons, and contaminating toluene and ether, respectively.

intermediate by measuring the ^{1}H NMR spectrum immediately after defrosting the solution that was prepared and frozen in liquid nitrogen (Figure 1a). The intermediate quickly disappeared as the solution warmed, and simultaneously, equivalent amounts of $\mathbf{1aH(1,4)}$ and $\mathbf{RuAN}^{2+}$ appeared. When $[Ru(tpy)(bpy)D]^+$ was used, the deuterium was exclusively incorporated at the 4-positions in the intermediate and then in the product without H/D exchange with protons in the reaction solution (Figure S1 in the Supporting Information). The intermediate was determined to be a 1:1 adduct of $[Ru(tpy)(bpy)]^{2+}$ and $\mathbf{1aH(1,4)}$ ($\mathbf{Ru1aH(1,4)}^{2+}$) based on kinetic studies of the reaction (*vide infra*) and ^{1}H NMR spectrum. In the IR spectrum of $\mathbf{Ru1aH(1,4)}^{2+}$ (Figure S2), the absorptions attributed to C=C stretching modes were observed at lower frequencies (1604 and 1685 cm^{-1}) compared with that of $\mathbf{1aH(1,4)}$ (1628 and 1695 cm^{-1}).[8]

Similar adduct formation was observed for the reaction of $\mathbf{RuH}^+$ with 1-methyl-3-trifluoromethylpyridinium ($\mathbf{1b}^+$) and 1-isopropyl-3-trifluoromethylpyridinium ($\mathbf{1c}^+$). The adducts $\mathbf{Ru1bH(1,4)}^{2+}$ and $\mathbf{Ru1cH(1,4)}^{2+}$ were converted to $\mathbf{1bH(1,4)}$ and $\mathbf{1cH(1,4)}$, respectively, with formation of $\mathbf{RuAN}^{2+}$ in quantitative yield (Figures S3 and S4).

The 1-benzylpyridinium cation ($\mathbf{1d}^+$) has no substituent at the 3-position, but it reacted with $\mathbf{RuH}^+$; however, the reaction was comparatively slow and was complete in about 12 h even at room temperature. It afforded a more stable intermediate species ($\mathbf{Ru1dH(1,4)}^{2+}$) with the formation of $\mathbf{1dH(1,4)}$ and an equivalent amount of $\mathbf{RuAN}^{2+}$ during the initial stage of the reaction, confirmed by an ^{1}H NMR spectrum immediately after PF_6^- salts of both $\mathbf{1d}^+$ (9 μmol) and $\mathbf{RuH}^+$ (8 μmol) were dissolved in 0.7 mL of acetonitrile-d_3 at room temperature (Figure S5a). A trace amount of another intermediate species ($\mathbf{Ru1dH(1,2)}^{2+}$, described below) was also detected (the inset of the same figure).

The structure of $\mathbf{Ru1dH(1,4)}^{2+}$ could be assigned to a 1:1 adduct of $[Ru(tpy)(bpy)]^{2+}$ and the 1,4-dihydro form of $\mathbf{1d}^+$ ($\mathbf{1dH(1,4)}$), in which the signals from the protons at 2- and 3-positions were observed at magnetic fields different from those at the 5- and 6-positions in the ^{1}H−^{1}H gradient-COSY spectrum (Figure S6). In an NOE experiment for $\mathbf{Ru1dH(1,4)}^{2+}$, two NOEs of the protons at the 5- and 6-positions of the $\mathbf{1dH(1,4)}$ unit with the proton at the 6-position of bpy in the Ru complex unit were observed with similar magnitude (Figure S7). In the following stage of the reaction, a decrease in $\mathbf{Ru1dH(1,4)}^{2+}$ and an increase in $\mathbf{1dH(1,4)}$ and $\mathbf{RuAN}^{2+}$ were mainly observed, while a small amount of another adduct ($\mathbf{Ru1dH(1,2)}^{2+}$) with the 1,2-dihydro form of $\mathbf{1d}^+$ ($\mathbf{1dH(1,2)}$) instead of the $\mathbf{1dH(1,4)}$ unit was produced (Figure S5b and the inset of Figure S5a). Finally, both of the adducts were dissociated to give $\mathbf{RuAN}^{2+}$ and the corresponding dihydro form, i.e., $\mathbf{1dH(1,4)}$ and $\mathbf{1dH(1,2)}$, in 94% and 3% yields, respectively (Figure S5c).

The ^{1}H NMR data of $\mathbf{Ru1aH(1,4)}^{2+}$ and $\mathbf{Ru1dH(1,4)}^{2+}$, along with the adduct of BNAH with $\mathbf{RuH}^+$ ($\mathbf{RuBNAH}^{2+}$), are summarized in Table S1.

The chemical shifts observed in the range from 0.7 to 6.4 ppm clearly indicate that the pyridinium rings were already reduced in the process of forming the adducts. Moreover, the pyridinium rings exhibited the 1,4-dihydro structure (except for $\mathbf{Ru1dH(1,2)}^{2+}$), which was established by the two doublets and two triplets that were observed for the protons on the dihydropyridine ring of the adducts. The ^{1}H NMR spectra of the adducts showed the following characteristics ($\mathbf{Ru1dH(1,4)}^{2+}$ is discussed as a typical example): (1) there were none of the magnetically equivalent protons of the dihydropyridine ring and those of the tpy ligand in the Ru complex, indicating that the adduct has C_1 symmetry; (2) geminal coupling of the protons at the 4-position was observed ($^2J \approx 20$ Hz), and both proton signals were observed at higher magnetic fields, where one was more strongly shielded (−2.02 ppm) than the other (−0.51 ppm); (3) geminal coupling of the methylene protons of the benzyl substituent at the 1-position was also observed, and shielding effects on the methylene protons were observed to different extents as well; (4) shielding effects were observed at the 2- and 5-positions (2-position, −0.87 ppm, 5-position, −0.60 and −0.54 ppm), whereas the proton at 6-position was deshielded (+0.64 ppm).

These results strongly indicate that the 1,4-dihydropyridine moiety coordinates to the Ru center with one of the C=C bonds in an η^2 mode but not by the N lone pair in η^1 mode because of the following reasons: (1) the W(0) complex having 1-acetyl-1,2-dihydropyridine as a ligand coordinated in an η^2 mode to the W(0) center via the C=C bond between the 3- and 4-positions has been reported,[8] and in the ^{1}H NMR spectrum of this complex, a similar geminal coupling of the methylene groups and similar magnetic shielding effects of the dihydropyridine protons were observed;[9] (2) the magnitude of shielding effects of the protons at the 4-position was obviously larger than that of $\mathbf{RuBNAH}^{2+}$, in which the carbamoyl group at

dx.doi.org/10.1021/om400862n | *Organometallics* 2013, 32, 6162−6165

the 3-position coordinates to the metal center and the protons at the 4-position are relatively close to the tpy ligand; (3) it seems reasonable that the π bonding encumbered free rotation of the dihydropyridine on the metal center, resulting in the C_1-symmetrical appearance of the dihydropyridine and the tpy protons of **Ru1dH(1,4)**$^{2+}$ in the NMR spectrum, as described above; (4) the shifts of the C=C stretching bands of **Ru1aH(1,4)**$^{2+}$ to lower frequencies (−24 and −10 cm^{-1}) indicate weak interactions in comparison with the reported shifts (−100 to −200 cm^{-1}) of η^2-form structures of $[Ru(NH_3)_5(alkene)]^{2+}$.[10] The binding position of the dihydropyridine rings to the Ru(II) center could be determined on the basis of NMR experiments. The NOE data of **Ru1dH(1,4)**$^{2+}$ indicate that the carbon atoms at both the 5- and 6-positions were located at similar distances from the metal center.

In **Ru1aH(1,4)**$^{2+}$−**Ru1cH(1,4)**$^{2+}$, the magnetic shielding effects of the protons at the 5- and 6-positions by binding to the $[Ru(tpy)(bpy)]^{2+}$ moiety (from −0.40 to −0.52 ppm and from +0.20 to +0.50 ppm, respectively) are similar to those for **Ru1dH(1,4)**$^{2+}$ (−0.54 and +0.64 ppm, respectively).

This similarity of the shielding effect is also applicable to all other protons. Thus, the 1,4-dihydropyridine moieties of the adducts **Ru1aH(1,4)**$^{2+}$−**Ru1dH(1,4)**$^{2+}$ exhibit the η^2-C(5)=C(6) binding mode as shown in Scheme 1.

Is the formation of the η^2 adducts the key to achieving regioselective hydride transfer to pyridinium cations? The reaction of **RuH**$^+$ with **1d**$^+$ offers a test case, since two isomers (**Ru1dH(1,4)**$^{2+}$ as a main product and **Ru1dH(1,2)**$^{2+}$ as a very minor product) were observed in the NMR experiment. Figure 2 shows the time courses of concentrations of **RuH**$^+$, **Ru1dH(1,4)**$^{2+}$, **Ru1dH(1,2)**$^{2+}$, **1dH(1,4)**, **1dH(1,2)**, and **RuAN**$^{2+}$ during the reaction of **RuH**$^+$ with **1d**$^+$, where the initial concentrations of **RuH**$^+$ and **1d**$^+$ were 6.0 and 6.3 mM, respectively. In the initial stage of the reaction, rapid formation of **Ru1dH(1,4)**$^{2+}$ and the corresponding decay of **RuH**$^+$ were observed, followed by comparatively slow changes in the concentrations. This behavior can be explained by an equilibrium reaction followed by an irreversible reaction to yield a product; the first reaction corresponds to formation of **Ru1dH(1,4)**$^{2+}$, and the irreversible reaction corresponds to the cleavage of **Ru1dH(1,4)**$^{2+}$. This kinetic model is supported by an analysis of a steady-state approximation (see section F in the Supporting Information for details).

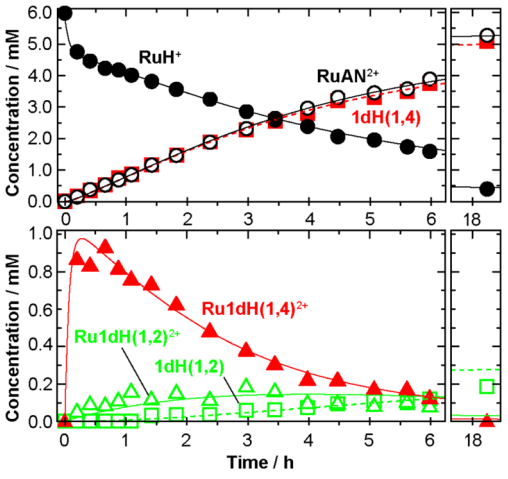

Figure 2. Concentrations of **RuH**$^+$ (black ●), **RuAN**$^{2+}$ (black ○), **1dH(1,4)** (red ■), **Ru1dH(1,4)**$^{2+}$ (red ▲), **Ru1dH(1,2)**$^{2+}$ (green △), and **1dH(1,2)** (green □) over time during the reaction of **RuH**$^+$ with **1d**$^+$ at 22 °C. The initial concentrations of **RuH**$^+$ and **1d**$^+$ are 6.0 and 6.3 mM, respectively. Fitting curves are based on a kinetic model using Scheme 2

Meanwhile, formation of **Ru1dH(1,2)**$^{2+}$ was observed as a very minor reaction without an induction period, while the formation of **1dH(1,2)** had an induction period (about 1 h). Since the formation of **1dH(1,2)** was observed after the formation of **Ru1dH(1,2)**$^{2+}$ and stopped after the disappearance of **Ru1dH(1,2)**$^{2+}$, **1dH(1,2)** is likely to have been formed via cleavage of **Ru1dH(1,2)**$^{2+}$ and not via isomerization of **1dH(1,4)**.[11]

There are two possible mechanisms to give **Ru1dH(1,2)**$^{2+}$ (Scheme 2): (A) direct formation from **1d**$^+$ and **RuH**$^+$ and/or

Scheme 2. Possible Reaction Pathways

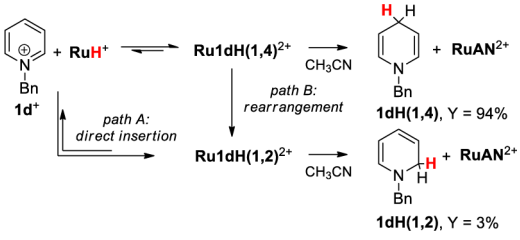

(B) rearrangement of the 1,4-dihydropyridine moiety in **Ru1dH(1,4)**$^{2+}$ to the 1,2-isomer on the $[Ru(tpy)(bpy)]^{2+}$ moiety. Path A seems reasonable as the major pathway, because no induction period was readily observed in Figure 2; on the other hand, an antarafacial [1,3]-sigmatropic shift such as path B would be sterically hindered. To clarify this, we tested the reaction using higher concentrations of **RuH**$^+$ (44 mM) and **1d**$^+$ (175 mM) and found that **Ru1dH(1,2)**$^{2+}$ was clearly formed without any induction period and, in the initial stage of the reaction, the ratio of **Ru1dH(1,4)**$^{2+}$ to **Ru1dH(1,2)**$^{2+}$ was 96:4 (Figure S9). This ratio, comparable to the product yields of **1dH(1,4)** and **1dH(1,2)** described above (94% and 3%, respectively), indicates that path A was operating. Therefore, the formation of the 1:1 adducts is the key stage to determine the regioselectivity of the free dihydropyridine products. Note that the reaction of **1d**$^+$ with **RuH**$^+$ involving both paths A and B was slower than the reactions of **1a**$^+$−**1c**$^+$.

To obtain further mechanistic insights into the reactions, we employed the stopped-flow technique to follow the formation of the adducts of **1a**$^+$−**1c**$^+$ with **RuH**$^+$ and the subsequent cleavage of **Ru1aH(1,4)**$^{2+}$−**Ru1cH(1,4)**$^{2+}$. Two-step spectral changes were observed, and in each step, there were isosbestic points (Figures S10−S12). These results are consistent with the results of the low-temperature NMR experiments as described above. In the first stage (<5 s), the metal-to-ligand charge-transfer absorption band of the Ru complex was blue-shifted (λ_{max} from 535 to 451 (**1a**$^+$), 443 (**1b**$^+$), and 465 (**1c**$^+$) nm); this is attributed to the formation of the adduct. The spectrum of the adduct subsequently changed to that of the solvento complex $[Ru(tpy)(bpy)(DMF)]^{2+}$ (λ_{max} 485 nm[12]) on a time scale of several tens to several hundreds of seconds; this is attributed to the cleavage of the adduct. Since in the adduct formation the observed pseudo-first-order rate constants were proportional to the concentrations of **1a**$^+$−**1c**$^+$, the second-order rate constants (k_2) for the reactions could be determined.

dx.doi.org/10.1021/om400862n | *Organometallics* 2013, 32, 6162−6165

Linear Arrhenius plots of k_2 obtained between 15 and 45 °C (Figures S13−S16) provided the kinetic activation parameters for the adduct formation, as summarized in Table S2.

These activation parameters are compared with those for the adduct formation of BNA^+ with $\mathbf{RuH}^+$,[4c] because the structures of $\mathbf{Ru1aH(1,4)}^{2+}$−$\mathbf{Ru1dH(1,4)}^{2+}$ are distinct from those of BNA^+ coordinated to Ru via the carbamoyl group. Interestingly, the activation entropies for the adduct formation are comparable to each other and have large negative values (about −100 J mol^{-1} K^{-1}). This strongly suggests that, in each type of adduct formation, there is an intermediate with a strictly packed structure, which can induce 1,4-regioselective hydride reduction of the pyridinium cation.

Although rare precedents for η^2 bonding of the heterocycle as observed in these intermediates are found in the chemistry of $[Os(NH_3)_5]^{2+}$,[13] W(0),[9a] and Ru(II),[14] to our knowledge, this is the first study to demonstrate such bond formation resulting from hydride-transfer reactions to yield the position-selective dihydro forms.

■ ASSOCIATED CONTENT

Supporting Information

Figures, tables, a detailed experimental section, characterization data, activation parameters, and stopped-flow analysis data. This material is available free of charge via the Internet at http://pubs.acs.org.

■ AUTHOR INFORMATION

Corresponding Author

*E-mail for O.I.: ishitani@chem.titech.ac.jp.

Present Address

[⊥]Research Institute for Innovation in Sustainable Chemistry, National Institute of Advanced Industrial Science and Technology (AIST), 1-1-1 Higashi, Tsukuba 305-8565, Japan.

Notes

The authors declare no competing financial interest.

■ ACKNOWLEDGMENTS

This work was supported by a Grant-in Aid for Exploratory Research (24655046) from the Ministry of Education, Culture, Sports, Science and Technology (MEXT). The research at Brookhaven National Laboratory (BNL) was conducted under contract DE-AC02-98CH10884 with the U.S. Department of Energy and supported by its Division of Chemical Sciences, Geosciences and Biosciences of the Office of Basic Energy Sciences. We thank Dr. Etsuko Fujita (BNL) for helpful comments.

■ REFERENCES

(1) (a) Wagenknecht, P. S.; Penney, J. M.; Hembre, R. T. *Organometallics* **2003**, *22*, 1180. (b) Fukuzumi, S.; Tanaka, T. In *Photoinduced Electron Transfer*; Fox, M. A., Chanon, M., Eds.; Elsevier: New York, 1988; Vol. *C*, p 578. (c) Murakami, Y.; Kikuchi, J.-i.; Hisaeda, Y.; Hayashida, O. *Chem. Rev.* **1996**, *96*, 721. (d) Ohno, A. In *Asymmetric Reactions and Processes in Chemistry*; American Chemical Society: Washington, DC, 1982; Vol. *185*, p 219. (e) Yasui, S.; Ohno, A. *Bioorg. Chem.* **1986**, *14*, 70.

(2) (a) Eisner, U.; Kuthan, J. *Chem. Rev.* **1972**, *72*, 1. (b) Kuthan, J.; Kurfurst, A. *Ind. Eng. Chem. Prod. Res. Dev.* **1982**, *21*, 191. (c) Lavilla, R. *J. Chem. Soc., Perkin Trans. 1* **2002**, 1141.

(3) (a) Carelli, V.; Liberatore, F.; Scipione, L.; Musio, R.; Sciacovelli, O. *Tetrahedron Lett.* **2000**, *41*, 1235. (b) Poddubnyi, I. S. *Chem. Heterocycl. Compd.* **1995**, *31*, 682. (c) Roberts, R. M. G.; Ostovic, D.; Kreevoy, M. M. *J. Org. Chem.* **1983**, *48*, 2053. (d) Blankenhorn, G.; Moore, E. G. *J. Am. Chem. Soc.* **1980**, *102*, 1092. (e) Klopman, G. *J. Am. Chem. Soc.* **1968**, *90*, 223. (f) Kosower, E. M.; Bauer, S. W. *J. Am. Chem. Soc.* **1960**, *82*, 2191. (g) Mauzerall, D.; Westheimer, F. H. *J. Am. Chem. Soc.* **1955**, *77*, 2261. (h) McSkimming, A.; Colbran, S. B. *Chem. Soc. Rev.* **2013**, *42*, 5439.

(4) (a) Soldevila-Barreda, J. J.; Bruijnincx, P. C. A.; Habtemariam, A.; Clarkson, G. J.; Deeth, R. J.; Sadler, P. J. *Organometallics* **2012**, *31*, 5958. (b) Shaw, A. P.; Ryland, B. L.; Franklin, M. J.; Norton, J. R.; Chen, J. Y. C.; Hall, M. L. *J. Org. Chem.* **2008**, *73*, 9668. (c) Kobayashi, A.; Takatori, R.; Kikuchi, I.; Konno, H.; Sakamoto, K.; Ishitani, O. *Organometallics* **2001**, *20*, 3361. (d) Konno, H.; Sakamoto, K.; Ishitani, O. *Angew. Chem., Int. Ed.* **2000**, *39*, 4061. (e) Hembre, R. T.; McQueen, S. *J. Am. Chem. Soc.* **1994**, *116*, 2141. (f) Collman, J. P.; Wagenknecht, P. S.; Lewis, N. S. *J. Am. Chem. Soc.* **1992**, *114*, 5665. (g) Matsubara, Y.; Fujita, E.; Doherty, M. D.; Muckerman, J. T.; Creutz, C. *J. Am. Chem. Soc.* **2012**, *134*, 15743.

(5) Ellis, W. W.; Raebiger, J. W.; Curtis, C. J.; Bruno, J. W.; DuBois, D. L. *J. Am. Chem. Soc.* **2004**, *126*, 2738.

(6) (a) Leiva, C.; Lo, H. C.; Fish, R. H. *J. Organomet. Chem.* **2010**, *695*, 145. (b) Lo, H. C.; Leiva, C.; Buriez, O.; Kerr, J. B.; Olmstead, M. M.; Fish, R. H. *Inorg. Chem.* **2001**, *40*, 6705. (c) Lo, H. C.; Buriez, O.; Kerr, J. B.; Fish, R. H. *Angew. Chem., Int. Ed.* **1999**, *38*, 1429. (d) Steckhan, E.; Herrmann, S.; Ruppert, R.; Dietz, E.; Frede, M.; Spika, E. *Organometallics* **1991**, *10*, 1568.

(7) Maenaka, Y.; Suenobu, T.; Fukuzumi, S. *J. Am. Chem. Soc.* **2012**, *134*, 9417.

(8) Kobayashi, A.; Konno, H.; Sakamoto, K.; Sekine, A.; Ohashi, Y.; Iida, M.; Ishitani, O. *Chem. Eur. J.* **2005**, *11*, 4219.

(9) (a) Harrison, D. P.; Zottig, V. E.; Kosturko, G. W.; Welch, K. D.; Sabat, M.; Myers, W. H.; Harman, W. D. *Organometallics* **2009**, *28*, 5682. (b) Alper, H. *J. Organomet. Chem.* **1975**, *96*, 95.

(10) Lehmann, H.; Schenk, K. J.; Chapuis, G.; Ludi, A. *J. Am. Chem. Soc.* **1979**, *101*, 6197.

(11) Although the rate of isomerization strongly depends on the type of substituent on the ring, solvent used, and temperature, the isomerization typically occurs over several days at room temperature: Fowler, F. W. *J. Am. Chem. Soc.* **1972**, *94*, 5926. Carelli, V.; Liberatore, F.; Tortorella, S.; Moracci, F. M. *Gazz. Chim. Ital.* **1983**, *113*, 569.

(12) Matsubara, Y.; Konno, H.; Kobayashi, A.; Ishitani, O. *Inorg. Chem.* **2009**, *48*, 10138.

(13) (a) Cordone, R.; Harman, W. D.; Taube, H. *J. Am. Chem. Soc.* **1989**, *111*, 2896. (b) Surendranath, Y.; Harman, W. D. *Dalton Trans.* **2006**, 3957.

(14) (a) Yamaguchi, S.; Shinokubo, H.; Osuka, A. *J. Am. Chem. Soc.* **2010**, *132*, 9992. (b) Chou, M. H.; Brunschwig, B. S.; Creutz, C.; Sutin, N.; Yeh, A.; Chang, R. C.; Lin, C. T. *Inorg. Chem.* **1992**, *31*, 5347. (c) Fish, R. H.; Fong, R. H.; Anh, T.; Baralt, E. *Organometallics* **1991**, *10*, 1209. (d) Chen, Y.; Lin, F.-T.; Shepherd, R. E. *Inorg. Chem.* **1997**, *36*, 818.